Cement & Concrete Composites 33 (2011) 506–512

Contents lists available at ScienceDirect

Cement & Concrete Composites

journal homepage: www.elsevier.com/locate/cemconcomp

A self-healing cementitious composite using oil core/silica gel shell microcapsules

Zhengxian Yang [a,c], John Hollar [a], Xiaodong He [a], Xianming Shi [a,b,*]

[a] Corrosion and Sustainable Infrastructure Laboratory, Western Transportation Institute, PO Box 174250, College of Engineering, Montana State University, Bozeman, MT 59717-4250, USA
[b] Civil Engineering Department, 205 Cobleigh Hall, Montana State University, Bozeman, MT 59717-2220, USA
[c] Materials and Environment, Faculty of Civil Engineering & Geosciences, Delft University of Technology, P.O. Box 5048, 2600 GA Delft, The Netherlands

ARTICLE INFO

Article history:
Received 6 December 2009
Received in revised form 3 December 2010
Accepted 29 January 2011
Available online 4 February 2011

Keywords:
Self-healing concrete
Microcapsules
Carbon microfibers
Cementitious composite

ABSTRACT

This paper presents work toward the development of a new family of self-healing materials that hold promise for "crack-free" concrete or other cementitious composites. This innovative system features the design of microcapsules with oil core and silica gel shell. Methylmethacrylate monomer and triethylborane were selected as the healing agent and the catalyst, i.e. oil core phases in the system. They were microencapsulated, respectively, through an interfacial self-assembly process and sol–gel reaction. Then the microcapsules were dispersed in fresh cement mortar along with carbon microfibers. The self-healing effect was evaluated using permeability measurements along with a fatigue test under uniaxial compression cyclic loading and further confirmed by surface analytical tools including optical microscope and field emission scanning electron microscope coupled with energy-dispersive X-ray analyzer (FESEM/EDX).

Published by Elsevier Ltd.

1. Introduction

With a smaller fracture energy relative to that of mild steel (about 0.1 kJ/m^2 vs. 100 kJ/m^2), cementitious materials are known to be inherently brittle and tend to crack under stress. Once microcracks form in concrete, they are difficult to detect and repair by conventional methods before they develop, coalesce and grow into macrocracks, which can pose a significant risk for the performance and service life of concrete. While better structural design, material selection and proportioning, and construction practices can help control concrete cracking, continued research in the domain of materials science (e.g., application of various fibers [1]) is crucial in improving the service life of concrete structures.

In recent years, the biomimetic concept of self-healing has been demonstrated for cementitious materials by incorporating healing agents in hollow porous fibers, or in hollow glass tubes with a brittle breakable sealer [2–6]. This concept has also been demonstrated for polymer composites [7,8], by dispersing the microencapsulated repairing agent and catalyst within the composite matrix phase, or by a bleeding action from filled hollow fibers [9]. As a response to applied heat or vacuum (active mode) or to mechanical loading (passive mode), the repairing chemicals (monomers) are released and repair the cracks or fill the voids often through polymerization [10].

The use of short fibers to reinforce cementitious composites seems to be a promising strategy in mitigating cracking at the microscale. Some composite systems with fiber reinforcement feature the strain-hardening behavior associated with the enhancement of tensile/flexural strength and toughness due to the combined actions of the fibers, cementitious matrix and their interface [11–14]. Owing to their small diameter and high aspect ratio, short fibers have a large numerical density in the matrix even when admixed at relatively low volume fractions and thus have the potential to interact with microcracks formed in cementitious composites [15]. As such, short fibers have been proven to effectively flank and bridge microcracks before they become coalescent and form macrocracks [16]. The admixing of short fibers in cementitious composites has shown many prospective benefits, especially in enhancing the self-healing capability of cementitious materials [17,18], but the effectiveness hinges on the uniform dispersion of fibers in the matrix.

This paper presents work towards the development of a new family of self-healing materials that are expected to offer potential synergy with microfibers in arresting cracks formed in concrete or other cementitious materials. The microfibers are expected to control the width of the cracks at the microscale in this work. This system we proposed herein features the design of microcapsules (PSMs) with oil core and silica gel shell, consisting of methylmethacrylate (MMA) as the healing agent and an initiator (catalyst) containing triethylborane (TEB). The healing agent and catalyst are microencapsulated respectively through an interfacial self-assembly process and sol–gel reaction [19,20]. More technical

* Corresponding author at: Corrosion and Sustainable Infrastructure Laboratory, Western Transportation Institute, PO Box 174250, College of Engineering, Montana State University, Bozeman, MT 59717-4250, USA. Tel.: +1 406 994 6486; fax: +1 406 994 1697.
E-mail address: Xianming_s@coe.montana.edu (X. Shi).

0958-9465/$ - see front matter Published by Elsevier Ltd.
doi:10.1016/j.cemconcomp.2011.01.010

details related to this process can be found in the following parts of this paper. The healing is designed to occur through a passive mode, i.e., as a response to crack propagation caused by cement hydration or external mechanical stimuli. The microcapsules are dispersed in fresh cement mortar along with carbon microfibers. For the hardened mortar, self-healing can be triggered by crack propagation through the microcapsules, which then releases the healing agent and the catalyst from their respective stress-ruptured reservoir upon crack intrusion. The monomer and its initiator have similar viscosity with water (i.e., dynamic viscosity is around 1.0 cP), so they can easily migrate into the microcracks through capillary action. Polymerization of the healing agent is then initiated by contact with the catalyst, bonding the crack faces.

2. Experimental

2.1. Materials

Commercially available monomers: styrene (St) and methylmethacrylate (MMA), poly(vinylpolypyrrolidone) (PVP), tetraethyl orthosilicate (TEOS), and concentrated sulfuric acid (98%) were obtained from Fisher Scientific Inc. Triethylborane solution (1.0M in hexanes) was obtained from Sigma–Aldrich, Inc. All the solvents were of analytical grade and were used as received. Deionized water was used for all experiments. The carbon microfibers were KRECA chop C-103T, 3 mm in length with a filament diameter of 18 μm, as obtained from Kureha Co. (Tokyo, Japan). In light of published work by other researchers [1,15], ASTM C1240 silica fume obtained from BASF/MB admixtures, Inc. (Henderson, NV), was used as a dispersant for the fibers in the mixes. ASTM C150-07 Type I/II low-alkali Portland cement was used in this study. The chemical composition and physical properties of the cement were presented in a previous reference [21]. The fine aggregate used was river sand sifted to allow a maximum aggregate size of 1.18 mm. Before proportioning and admixing, the aggregate was pretreated and taken to a saturated surface dry (SSD) condition.

2.2. Preparation of the PSMs

The overall preparation procedure of the PSMs is illustrated in Fig. 1. The first step was to self-assemble surface-sulfonated polystyrene particles at the water–oil droplet interface. The oil phase, either methylmethacrylate (MMA) monomer or triethylborane (TEB) solution (1.0M in hexane), was microencapsulated following the same procedure. The surface-sulfonated polystyrene particles of 0.7 ± 0.5 μm in diameter were prepared as reported previously [20] and the sulfonation time of polystyrene particles was 60 h for this study. After some preliminary trials, 0.15 g of the sulfonated polystyrene particles were dispersed into 45 ml deionized water using a high-intensity ultrasonic vibracell processor operated at 20 kHz and up to 10 W for 2 min to form a homogeneous system. Then 3 g of oil phase (oil/TEOS = 17/3, mol/mol) was introduced and stirred continuously using a magnetic stirrer operated at 500 rpm under the nitrogen atmosphere. The turbid mixture gradually evolved into a creamy-white emulsion in appearance after 20 min. Then the sample was set aside for 24 h.

During the reserving period, the TEOS tended to diffuse into the interface of oil phase and water, leading to hydrolysis and condensation reactions of alkoxysilane precursors that were catalyzed by surface sulfogroup of the sulfonated polystyrene particles. After 24 h, microcapsules with oil core and silica gel shell were formed and at the same time the adsorbed polystyrene particles disengaged from the shell. The microcapsules with MMA oil core were used as reservoirs for healing agent, while the microcapsules with TEB oil core were used as reservoirs for chemical initiator (catalyst) in this system.

2.3. Preparation of mortar specimens

Three types of carbon microfiber-reinforced mortar specimens including the control (with no particles admixed), the sulfonated polystyrene modified mortars (SPSM, with sulfonated polystyrene particles admixed), and the self-healing mortars (SHM, with microcapsules admixed) were investigated. For each type of mortars, three or more specimens were fabricated for each planned test to ensure the statistical reliability of the test results. The carbon microfiber content in the mortar mix was 2.0% by volume. The silica fume content was 15% by weight of binder. All specimens were prepared in an ordinary mortar mixer at a constant water-to-binder mass ratio of 0.52 and a constant sand-to-binder mass ratio of 2. The mixing sequence was the following: the cement, silica

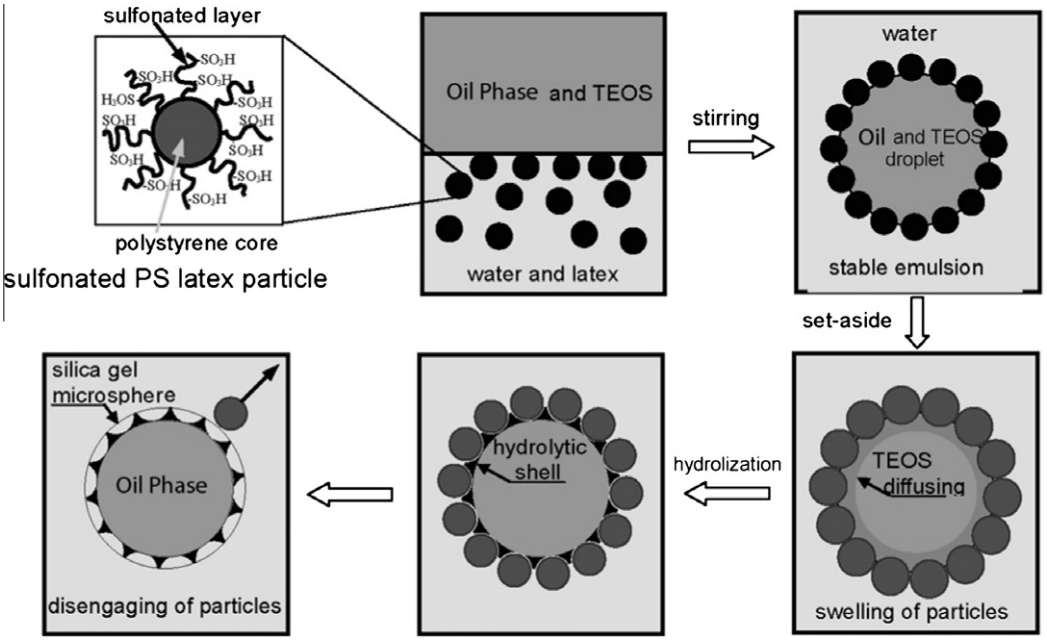

Fig. 1. Schematic illustration of the formation of the passive smart microcapsules.

fume, and mixing water were first mixed to form a paste, and then the fibers were slowly added while mixing continued, and finally the sand was incorporated. For the sulfonated polystyrene modified mortar specimens, a homogeneous solution containing 0.15% (by weight of cement) sulfonated polystyrene particles was used as the mixing water. For the self-healing mortar specimens, a freshly prepared solution containing 1.5% (by weight of cement) microcapsules with MMA oil core was mixed into cement and then stirred thoroughly for 5 min. Afterwards, a freshly prepared solution containing 0.03% (by weight of cement) microcapsules with TEB oil core was added into the mixture and stirred thoroughly for another 5 min. The total content of sulfonated polystyrene particles dispersed in the two solutions above for preparing PSMs was 0.15% by weight of cement. Since the amount of sulfonated polystyrene particles admixed in SPSM and SHM mortar specimens was kept consistent, the SPSM specimens were used as the second control relative to the SHM specimens. After mixing, the fresh mixture was cast into molds to form Φ50 mm × 100 mm cylinders, and was carefully compacted to minimize the amount of entrapped air. The mortar specimens were de-molded after 24 h and then cured in a wet chamber (relative humidity in excess of 95%, temperature 20 ± 2 °C) for 27 additional days.

2.4. Characterization and testing of materials

2.4.1. Optical and FESEM imaging of the PSMs and particles

In order to confirm that the healing agent (MMA) and the catalyst (TEB) were successfully microencapsulated, an organic fluorescent dye, 2,7-bis (N,N-diphenylamino)-9,9-diethyl-fluorene, was incorporated into the oil phase (5 mg/ml) and then was introduced to the reaction system to prepare the microcapsules. At the completion of the PSMs fabrication, an Olympus BX61 optical microscope and a Zeiss Supra 55VP PGT/HKL FESEM system were employed to examine the morphology of the PSMs and surface-sulfonated polystyrene particles.

2.4.2. Permeability test of mortar specimens

The permeability of concrete is one of the most important microstructural properties directly related to its durability and long-term performance. Among many techniques that could be performed to measure the permeability of cement composite, gas permeability using liquid methanol as the gas source is one of the easiest and fastest [22–25]. In this study, we used the apparatus and approach proposed by Alshamsi and Imran [25] to determine the permeability coefficient of the mortar specimens after being subjected to compression loading. Specimens at 1-day and 28-day curing ages from three types of prepared Φ50 mm × 100 mm cylinders were selected to conduct this test. Firstly, they were loaded under 80% of their respective ultimate compressive strength and then set aside for 24 h. After that, three 10 mm-thick cylindrical disk specimens were cut from the middle of the cylinders. Subsequently, the disk specimens were vacuum-dried at room temperature for 24 h to remove the moisture within specimens and then placed and sealed on the top of a cell with epoxy sealer to avoid leakage of methanol vapor as shown schematically in Fig. 2.

The initial weight of the whole specimen setup including the cell, methanol liquid, and disk specimen and epoxy sealer was measured at the beginning of the test. The values of mass variation vs. time due to the vaporization of methanol liquid at a constant 40 °C water bath temperature during the test were continuously recorded at each time interval until a steady-state mass loss was reached. Fig. 3 provides a typical plot of the gas permeability test data. The permeability coefficient was then calculated using the following equations [25–27].

$$p_V = 10^{\left(8.0809-\frac{1582.2}{239.76+T}\right)}$$

$$\eta = 10^{-7}\left(4.7169T^{0.618} - 99e^{-8.7593\times10^{-4}T} + 94e^{-7.916\times10^{-3}T} + 5\right)$$

$$Q = \frac{266\times10^{-3}m'}{10^{\left(8.0809-\frac{1582.2}{239.76+T}\right)}}T$$

$$k = \frac{2L\eta P_2 Q}{A\left(P_1^2 - P_2^2\right)}$$

where p_V = the absolute pressure of vapor (N/m^2), T = the absolute temperature (K), η = the dynamic viscosity (Ns/m^2), Q = the volumetric flow rate (m^3/s), m' = the rate of mass loss (g/s), k = the intrinsic permeability coefficient (m^2), P_1 = the inlet pressure (N/m^2), P_2 = the outlet pressure (N/m^2), L = the length of the sample (m) and A = the cross-sectional area perpendicular to the flow direction (m^2).

2.4.3. Fatigue test under uniaxial compression cyclic loading

The cylindrical mortar specimens were first loaded to 80% of their static ultimate compressive strength using a hydraulic Material Testing System (MTS Model 880) and then set aside for 24 h before being subjected to cyclically loading between 25% and 95% of their static ultimate compressive strength until failure. Fatigue strain data was recorded using a strain gage from Vishay Micro-Measurements group, Inc. (Raleigh, NC). Because the maximum aggregate size used was 1.18 mm in diameter, a gage length of 6.35 mm (larger than the minimum recommendation of 5.89 mm) was deemed sufficient. The frequency of loading was 1 Hz, and was applied sinusoidally with time. Data was recorded using a Campbell Scientific® CR5000 data-logger. A Tektronix® CPS250

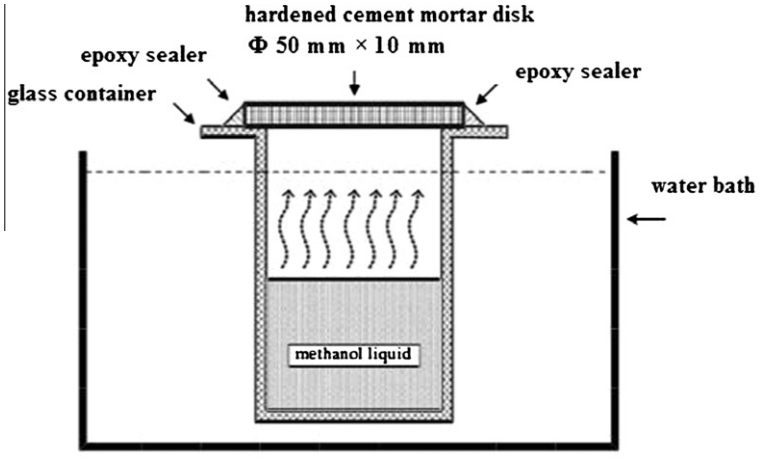

Fig. 2. Schematic illustration of experimental setup for the gas permeability test.

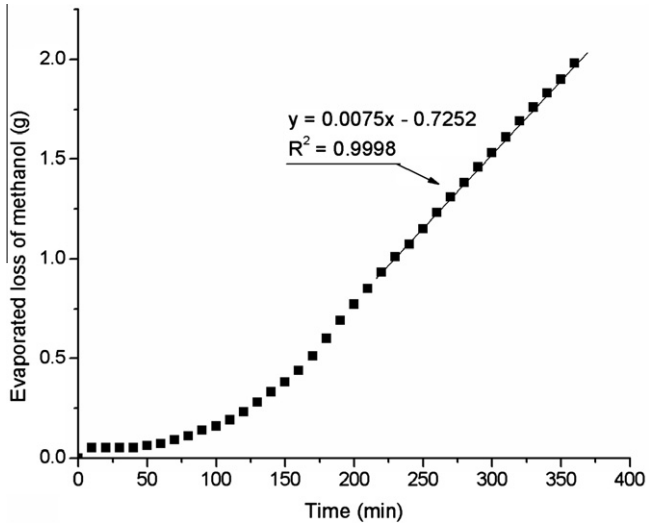

Fig. 3. Typical relationship between time and evaporated mass loss of methanol during gas permeability test.

power supplier was used to supply power to the strain gage circuitry.

2.4.4. Microscopic observation of microcracks and FESEM/EDX analyses

For surface analysis of microcracking and self-healing behavior in mortar, the specimen was loaded under 80% ultimate compressive strength to generate some artificial microcracks. Afterwards, a cylindrical disk was cut directly from the middle of the cylinder and then set aside for 24 h before being subjected to a Zeiss Supra 55VP PGT/HKL FESEM/EDX system to examine its localized morphology and elemental distributions at the microscopic level. The EDX data was obtained using a micro-analytical unit that featured the ability to detect the small variations of trace element content.

3. Results and discussion

3.1. Self-healing concept of the PSMs in mortar

The concept of self-healing of the PSMs in cement mortar is illustrated in Fig. 4. When a microcrack is initiated due to mechanical stress, it is expected to rupture the microcapsules by crack propagation and thus release both the healing agent and the catalyst. The healing agent fills into the cracks through capillary action. When the healing agent is in contact with the catalyst through the cracked microcapsules, its polymerization is triggered to bond the crack faces together. To enable the polymerization of MMA at room temperature and in the presence of oxygen-containing air, we chose the catalyst system as shown in Fig. 5 [28,29].

3.2. Morphology of the PSMs and particles

Optical microscopic images of the PSMs are shown in Fig. 6a and b as an overlay of the transmission bright field image and the fluorescent image, which clearly indicate the encapsulation of the oil phase including healing agent (MMA) or catalyst (TEB) along with the fluorescent dye by the silica microcages. We used the Adobe Photoshop CS4 software to measure at least 100 droplets in the optical photos and revealed that the diameter of the two types of PSMs featured an average diameter of 4.15 μm.

The morphology of microcapsules and surface-sulfonated polystyrene particles was further examined by FESEM as shown in Fig. 7a and b. While most microcapsules featured completely closed shells, a small amount of microcapsules with open pores

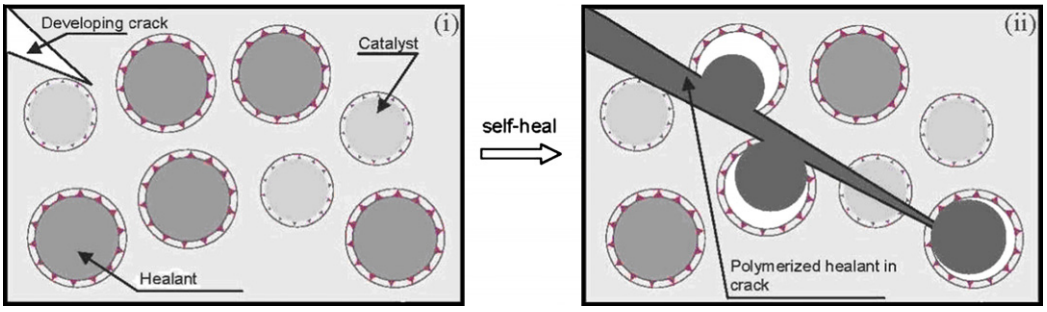

Fig. 4. Schematic illustration of the self-healing concept. (i) Healing agent and catalyst encapsulated in PSMs are dispersed in cementious material and microcrack is forming. (ii) The crack ruptures the microcapsules and the healing agent contacts the catalyst, triggering polymerization that bonds the crack faces.

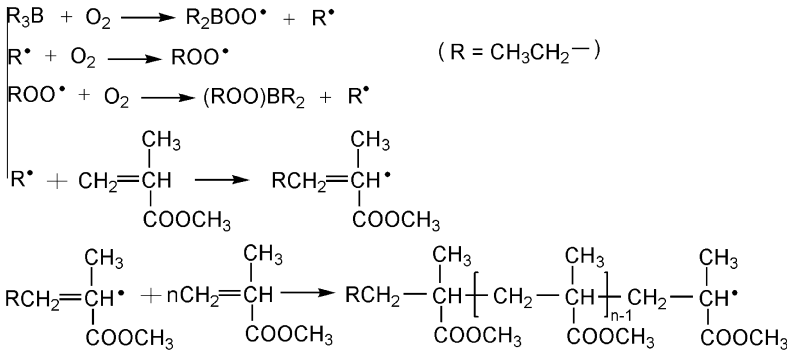

Fig. 5. Radical polymerization of methylmethacrylate initiated by triethylborane at room temperature.

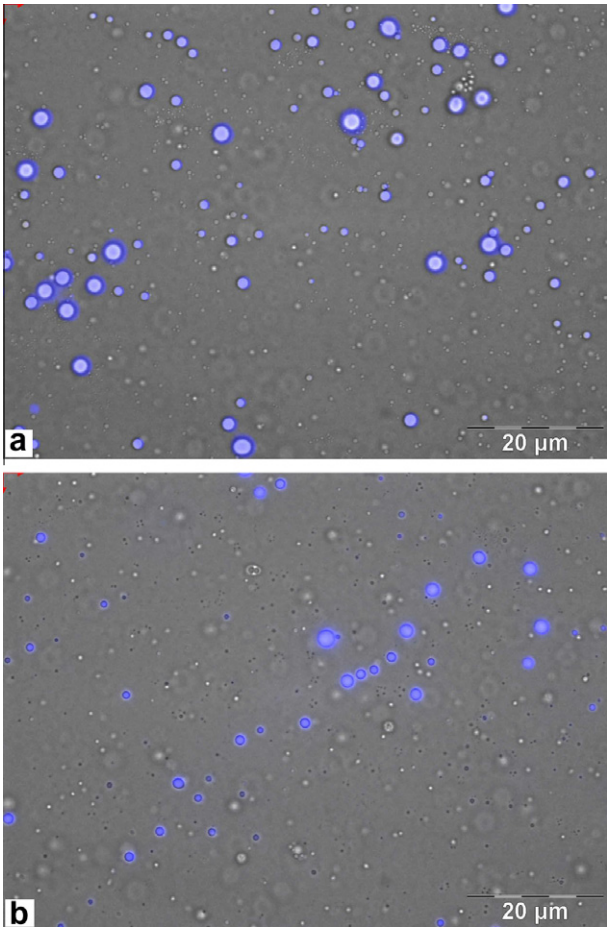

Fig. 6. Optical microscopic images of (a) MMA healing-agent-containing microcapsules and (b) TEB catalyst-containing microcapsules.

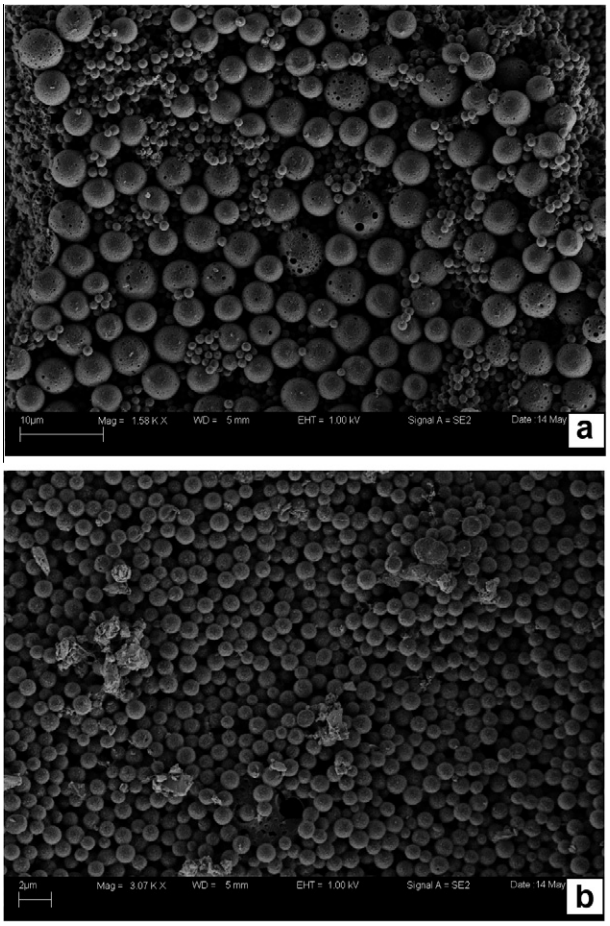

Fig. 7. FESEM images of: (a) the composite microcapsules and (b) surface-sulfonated polystyrene particles.

on the shell were also observed. The closed and open state of the pores was adjusted using polystyrene particles subjected to different durations of sulfonation. The increase in sulfonation time increased the polarity of the microspheres surface, which in turn decreased the contact area of the latex particles at the surface of the oil droplet. As such, when the latex particles disengaged themselves from the silica gel shell, they left behind more closed microcapsules. In this study, the microcapsules with closed shells were successfully obtained using polystyrene particles sulfonated for 60 h.

3.3. Gas permeability of cement mortars

Fig. 8 shows the results of permeability coefficients of cement mortar composite at 3-day and 30-day curing ages, after being loaded under 80% of ultimate compressive strength and subsequently set aside for 24 h to allow the released healing agent to polymerize. Relative to the control, it can be seen that the highest percentage of decrease in the permeability coefficient was 50.2% and 66.8% for the self-healing mortar (SHM) at ages of 3 days and 30 days respectively. For the sulfonated polystyrene modified mortar (SPSM), a smaller percentage of decrease in the permeability coefficient was observed, i.e., 23.8% and 24.0% at ages of 3 days and 30 days respectively. Relative to the SPSM, the more highly reduced permeability of SHM can be attributed to the self-healing effect of PSMs. The results suggest that that with the help of carbon microfibers in controlling the crack width, the inclusion of PSMs

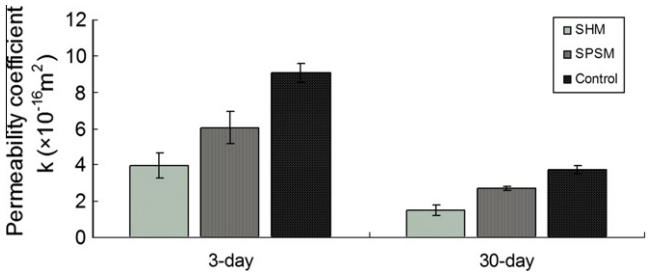

Fig. 8. Permeability coefficients of cement mortar composite at 3-day and 30-day curing ages, after being loaded under 80% of ultimate compressive strength and subsequently set aside for 24 h.

provided cement mortar with the ability to heal microcracks and to partially regain its mechanical properties.

In addition to the self-healing effect, we hypothesize that there are multiple mechanisms at work that account for why both types of microparticles reduced the permeability of cement mortar containing carbon microfibers and silica fume. First of all, these microparticles especially the PSMs, along with the silica fume particles are expected to assemble around the surface of carbon microfibers via physico-chemical interactions, facilitating the dispersion of microfibers in the cementitious matrix. Secondly, these microparticles can participate in the cement hydration process at the microscale and thus lead to less permeable microstructure of the hydrated cement. For PSMs, their silica gel shell can participate

in the pozzalanic reactions of cement hydration. Strong bonding between the microcapsules and the cementitious matrix can be expected as a result of the high contact area between the two phases. Finally, these microparticles can serve as micro-fillers and fill in the voids within the hydrated cement paste and at the interface of cement paste and fibers, leading to less permeable microstructure of the cementitious composite.

3.4. Fatigue behavior of the mortar specimens

Fatigue is progressive and permanent internal damage in a material subjected to repeated loading. This is attributed to the propagation of internal microcracks which results in a significant increase of irrecoverable strain. Previous studies have found that the addition of fibers can benefit the fatigue performance of concrete [30]. However, the benefit derived from the addition of fibers is not as significant under compressive fatigue loading as that under the flexural fatigue loading. Additionally, it has been suggested that the presence of fibers only help to enhance the fatigue behavior in low cycle regions and is limited in providing any improvement at a higher number of cycles [31,32]. In this study, the typical fatigue behavior of the microfiber-reinforced mortar specimens (SHM, SPSM, vs. control) under uniaxial compression cyclic loading was depicted by the relationship between the fatigue strain and the number of loading cycles until failure. As shown in Fig. 9, for all three types of mortar specimens, the fatigue strain development featured three distinct stages: the first stage characteristic of quick strain increase up to approximately 10% of the total life, the second stage characteristic of gradual strain increase from approximately 10–80% of the total life (attributed to the development of a large amount of small cracks in the mortar matrix), and the last stage characteristic of another quick strain increase until failure. Relative to the control, the SPSM and SHM specimens showed a significant prolonged second stage and their strain increment curves were less steep, demonstrating the beneficial role of these special microparticles in inhibiting the initiation and propagation of cracks. This also translates to higher load carrying capacity of microfiber-reinforced mortar specimens when they are admixed with PSMs and sulfonated polystyrene microspheres. Compared with the SPSM specimen, the SHM specimen showed smaller fatigue strain after the same number of load cycles, attributable to the self-healing effect of PSMs on enhancing the toughness of the cementitious composite under fatigue loading.

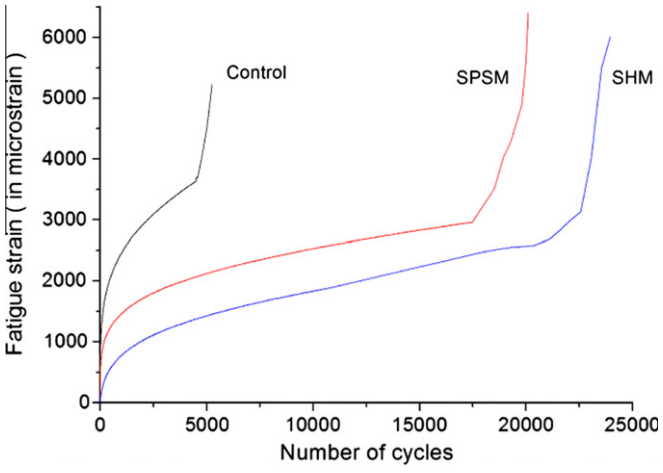

Fig. 9. Relationship between the fatigue strain and the number of cycles under uniaxial compression cyclic loading, for SHM, SPSM and control for control mortar specimens respectively.

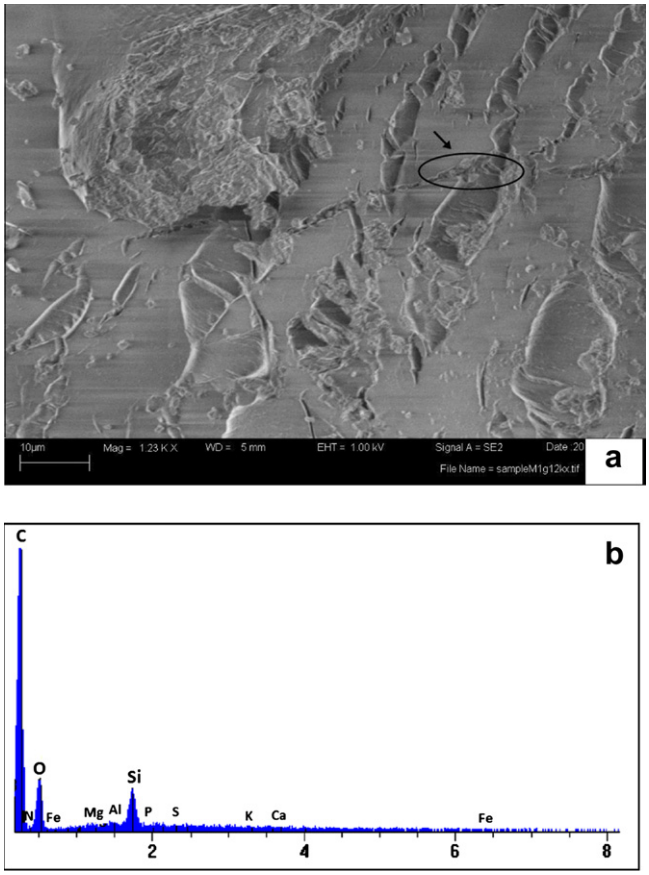

Fig. 10. (a) FESEM image of cracked surface of a SHM specimen; (b) The EDX spectrum showing the chemical composition of the area containing the microcracks on the SHM specimen surface.

3.5. Microscopic analyses

Recent technological advances in FESEM enable observations to be performed under a weak vacuum and thus allow for better maintenance of specimen microstructure. FESEM coupled with EDX provided information on the surface and thus shed light on the localized morphology and chemical composition of cracked areas.

The image of Fig. 10a was taken from surface of SHM specimen which was loaded under 80% ultimate compressive strength at 28 days and then subsequently set aside for 24 h. It can be found that some ruptured microcapsules existed and filled into the voids of cracks (as indicated by the arrowhead). Fig. 10b is the EDX spectrum showing the chemical composition of the area containing the microcracks on the surface of SHM specimen at a depth of approximately 1 μm from the surface to the mortar bulk matrix. The EDX data indicate that the surface of cracked area mainly consisted of C, O and Si, suggesting that the void of the cracks was filled mainly with PMMA and some cracked silica gel shell. The signal of boron (B) might be derived from the presence of the chemical initiator, triethylborane (TEB). In addition, the relative elemental content of C to O in cracks (58.0 wt.% vs. 20.8 wt.%) was similar to that of PMMA (67.6 wt.% vs. 22.5 wt.%), indicating the release of healing agent (MMA) by the externally applied mechanical force, and its polymerization in the 24 h subsequent to the compressive loading.

4. Conclusions

We proposed and investigated the concept of self-healing cementitious composite using oil core/silica gel shell microcap-

sules. Optical microscope and FESEM images revealed the microcapsules (PSMs) with closed shells and an average diameter of 4.15 μm were fabricated using polystyrene particles sulfonated for 60 h, and at the same time the oil phase including healing agent (MMA) and catalyst (TEB) was successfully encapsulated. The sulfonated polystyrene particles or PSMs were incorporated into the fresh cement mortar along with carbon microfibers and silica fume.

Gas permeability coefficients of cement mortar composite at different curing ages were studied, after being loaded under 80% of ultimate compressive strength and subsequently set aside for 24 h. Relative to the control, the highest percentage of decrease in the permeability coefficient was 50.2% and 66.8% for the self-healing mortar (SHM) at ages of 3 days and 30 days respectively. The inclusion of both types of microparticles was demonstrated to reduce the gas permeability of hydrated cement mortar composite. For the SHM, the reduced permeability can be partly attributed to the self-healing effect of PSMs. The crack resistance of the self-healing composites was also evaluated using a fatigue test under uniaxial compression cyclic loading. The test results revealed that the incorporation of a small dosage of PSMs into carbon microfiber-reinforced mortar improved the crack resistance and toughness of the specimens under fatigue loading. The self-healing effect was further confirmed by field emission scanning electron microscope coupled with energy-dispersive X-ray analyzer (FESEM/EDX).

This investigation demonstrated the feasibility of self-healing cementitious composites using oil core/silica gel shell PSMs. Such knowledge contributes to the search for effective measures to heal the microcracks in cementitious composites and thus reduce further damage of cement-based components or structures. Additional research is needed to further improve the healing efficiency, long-tem performance, and cost-effectiveness of this system.

Acknowledgements

This work was supported by the Research and Innovative Technology Administration under US Department of Transportation through the University Transportation Center research grant. The authors would like to extend their appreciation to Dr. Zhiyong Suo for the gift of fluorescent dye and helpful discussions and Dr. Recep Avci of the Imaging and Chemical Analysis Laboratory at Montana State University for the use of FESEM/EDX and optical microscopy instrumentation.

References

[1] Chung DDL. Cement reinforced with short carbon fibers: a multifunctional material. Composites Part B 2000;31(6–7):511–26.
[2] Dry C. Alteration of matrix permeability, pore and crack structure by the time release of internal chemicals. In: Proceedings: advance in cementitious materials. Gaithersbury, Maryland: American Ceramic Society; 1990. p. 729–68.
[3] Dry C. Three-part methylmethacrylate adhesive system as an internal delivery system for smart responsive concrete. Smart Mater Struct 1996;5(3):297–300.
[4] Li VC, Lim YM, Chan Y-M. Feasibility study of a passive smart self-healing cementitious composite. Composites Part A 1998;29(6):819–27.
[5] Dry C. Three designs for the internal release of sealants, adhesives, and waterproofing chemicals into concrete to reduce permeability. Cem Concr Res 2000;30(12):1969–77.
[6] Bleay SM, Loader CB, Hawyes VJ, Humberstone L, Curtis PT. Smart repair system for polymer matrix composites. Composites Part A 2001;32(12):1767–76.
[7] White SR, Sottos NR, Geubelle PH, Moore JS, Kessler MR, Sriram SR, et al. Autonomic healing of polymer composites. Nature 2001;409(6822):794–7.
[8] Brown EN, White SR, Sottos NR. Microcapsule induced toughening in a self-healing polymer composite. J Mater Sci 2004;39(5):1703–10.
[9] Pang JWC, Bond IP. A hollow fiber reinforced polymer composite encompassing self-healing and enhanced damage visibility. Compos Sci Technol 2005;65(11–12):1791–9.
[10] Dry C. Matrix cracking repair and filling using active and passive modes for smart timed release of chemicals from fibers into cement matrices. Smart Mater Struct 1994;3(2):118–23.
[11] Lange DA, Ouyang C, Shah SP. Behavior of cement based matrices reinforced by randomly dispersed microfibers. Adv Cem Based Mater 1996;3(1):20–30.
[12] Yi CK, Ostertag CP. Strengthening and toughening mechanisms in microfiber reinforced cementitious composites. J Mater Sci 2001;36(6):1513–22.
[13] Lawler JS, Zampini D, Shah SP. Permeability of cracked hybrid fiber-reinforced mortar under load. ACI Mater J 2002;99(4):379–85.
[14] Ahmed SFU, Mihashi H. A review on durability properties of strain hardening fiber reinforced cementitious composites (SHFRCC). Cem Concr Compos 2007;29(5):365–76.
[15] Fu X, Chung DDL. Self-monitoring of fatigue damage in carbon fiber reinforced cement. Cem Concr Res 1996;26(1):15–20.
[16] Ostertag CP, Yi CK. Crack/fiber interaction and crack growth resistance behavior in microfiber reinforced mortar specimens. Mater Struct 2007;40(7):679–91.
[17] Qian S, Zhou J, de Rooij MR, Schlangen E, Ye G, van Breugel K. Self-healing behavior of strain hardening cementitious composites incorporating local waste materials. Cem Concr Compos 2009;31(9):613–21.
[18] Qian S, Zhou J, Schlangen E. Influence of curing condition and precracking time on the self-healing behavior of engineered cementitious composites. Cem Concr Compos 2010;32(9):686–93.
[19] He X, Ge X, Liu H, Zhou H, Zhang Z. Self-assembly of latex particles at droplet interface to prepare monodisperse emulsion droplets. Colloids Surf A Physicochem Eng Aspects 2007;301(1–3):80–4.
[20] He X, Ge X, Liu H, Wang M, Zhang Z. Cagelike polymer microspheres with hollow core/porous shell structures. J Polym Sci Part A Poly Chem 2007;45(5):933–41.
[21] Yang Z, Shi X, Creighton AT, Peterson MM. Effect of styrene-butadiene rubber latex on the chloride permeability and microstructure of Portland cement mortar. Constr Build Mater 2009;23(6):2283–90.
[22] Cabrera JG, Lynsdale CJ. A new gas permeameter for measuring the permeability of mortar and concrete. Mag Concr Res 1988;40(144):177–82.
[23] Hoseini M, Bindiganavile V, Banthia N. The effect of mechanical stress on permeability of concrete: a review. Cem Concr Compos 2009;31(4):213–20.
[24] Picandet V, Khelidj A, Bastian G. Effect of axial compressive damage on gas permeability of ordinary and high-performance concrete. Cem Concr Res 2001;31(11):1525–32.
[25] Alshamsi AM, Imran HDA. Development of a permeability apparatus for concrete and mortar. Cem Concr Res 2002;32(6):923–9.
[26] Chang T-P, Shih J-Y, Yang K-M, Hsiao T-C. Material properties of portland cement paste with nano-montmorillonite. J Mater Sci 2007;42(17):7478–87.
[27] Dhir RK, Hewlett PC, Chan YN. Near surface characteristics of concrete: intrinsic permeability. Mag Concr Res 1989;41(147):87–97.
[28] Erdyakov SY, Mel'nik OA, Gurskii ME, Ignatenko AV, Vygodskii YS. New efficient boron containing initiators of methyl methacrylate radical polymerization. Russ Chem Bull Int Ed 2004;53(10):2215–20.
[29] Welch FJ. Polymerization of methyl methacrylate by triethylboron-oxygen mixtures. J Polym Sci 1996;61(171):243–52.
[30] Lee MK, Barr BIG. An overview of the fatigue behavior of plain and fiber reinforced concrete. Cem Concr Res 2004;26(4):299–305.
[31] Hsu TTC. Fatigue and microcracking of concrete. Mater Struct 1984;17(97):51–4.
[32] Yin W, Hsu TCC. Fatigue behavior of steel fiber reinforced concrete in uniaxial and biaxial compression. ACI Mater J 1995;92(1):71–81.